CHEMISTRY
A EUROPEAN JOURNAL

DOI: 10.1002/chem.201000249

Hybrid Porous Materials with High Surface Area Derived from Bromophenylethenyl-Functionalized Cubic Siloxane-Based Building Units

Watcharop Chaikittisilp, Ayae Sugawara, Atsushi Shimojima, and Tatsuya Okubo*[a]

Abstract: Sonogashira cross-coupling of bromophenylethenyl-terminated cubic, double four-ring, siloxane cages with di-/triethynyl compounds results in microporous poly(ethynylene aryleneethenylene silsesquioxane) networks, simply termed as polyorganosiloxane networks (PSNs). In comparison with porous organic polymers reported previously, these PSNs show relatively high surface area and comparable thermal stability. Their apparent BET specific surface areas vary in the range of 850–1040 $m^2 g^{-1}$ depending on the length and the connectable sites of the ethynyl compounds. Analyses of pore size distribution revealed bimodal micropores with relatively narrow distribution. The degree of cross-linking affects the degree of cleavage of the siloxane bonds, and this suggests that partial cleavage of the siloxane cages is mainly a result of cage distortion. Hydrogen adsorption was performed to evaluate potential of the PSNs as hydrogen storage media. Uptakes of up to 1.19 wt% at 77 K and 760 Torr and initial isosteric heats of adsorption as high as 8.0 kJ mol^{-1} were observed. These materials have been obtained by a combination of structural, synthetic organic, and materials chemistry, which can exploited to synthesize porous hybrid materials with specifically designed structures and functions.

Keywords: cross-coupling · hydrogen storage · microporous materials · organic–inorganic hybrid composites · siloxanes

Introduction

Zeolite and sol–gel-derived silica are representative classes of silica-based nanoporous materials with practical use for catalysis and separation in the chemical industry.[1,2] In particular, crystalline zeolites having molecular-sieve properties show great performance as shape-selective catalysts and separation membranes. Utilization of zeolites in emerging applications such as enantioselective catalysis and optoelectronics, however, has been constrained by difficulties in functionalization of their inorganic frameworks.[1b,3] Designed synthesis of zeolites with tailored microporosity and functionality has been impossible, partly due to a lack of understanding of their crystallization mechanisms.[4] In addition, although they are formed as thermodynamically metastable phases, their phase selection occurs under kinetic control. Thus, the products that crystallize under particular conditions are hardly predictable.[5] On the contrary, the surfactant-directed self-assembly process has been well studied as a route to control mesostructures of sol–gel-derived mesoporous silica, which can be achieved under both thermodynamic and kinetic control.[6] Sol–gel-derived silica can be functionalized by introduction of organosilanes containing organic moieties with desired functionality.[7] However, there are still difficulties in controlling local or atomic structures of sol–gel-derived silica networks, because such amorphous networks are formed randomly on the hydrolysis and polycondensation of the precursors. Progress toward locally ordered structures has been made in recent years, mainly by self-assembly of well-defined oligomers as molecular building units.[8–12]

Among oligomeric siloxane units, the cubic octameric siloxane cage Si_8O_{12}, commonly termed double four-ring (D4R), is of particular interest as an ideal molecular building unit because of its rigidity, hyperbranched architecture, high symmetry, and ease of functionalization.[13] D4R moieties bearing specific functional groups such as aldehyde, carboxyl, and epoxy have been used in diverse forms as model catalysts, components for polymer blends, organic light-emitting diodes, and so on.[14] Early attempts to construct silica-based micro- and/or mesoporous materials with molecular

[a] W. Chaikittisilp, Dr. A. Sugawara, Prof. Dr. A. Shimojima, Prof. Dr. T. Okubo
Department of Chemical System Engineering
The University of Tokyo
7-3-1 Hongo, Bunkyo-ku, Tokyo 113-8656 (Japan)
Fax: (+81) 3-5800-3806
E-mail: okubo@chemsys.t.u-tokyo.ac.jp

Supporting information for this article is available on the WWW under http://dx.doi.org/10.1002/chem.201000249.

homogeneity from predefined D4R units involved surfactant-directed co-assembly of D4R cages,[9] cross-linking of D4R units by hydrosilylation,[10] polycondensation of alkoxysilylated cages,[11] and self-assembly of well-designed amphiphilic molecules containing D4R cages.[12] Although claims were made that D4R units were retained in the siloxane networks, control over the microscopic arrangement of the cages and subsequent micropore size distribution remains to be achieved.

Recently, synthesis of microporous covalent organic polymers has advanced very rapidly, partly due to the urgent need for low-density porous materials for hydrogen and methane storage.[15–22] Such polymers, consisting solely of light elements (H, B, C, N, O, etc.), can be constructed by a wide variety of standard synthetic strategies in organic chemistry. In extreme cases, covalent organic frameworks (COFs) with crystalline structures and high surface area can be constructed under thermodynamic control.[16] The COFs are obtained by carefully selecting the building blocks and the conditions of their synthesis, which is carried out in a closed system to ensure reversibility of the condensation reactions; the choice of solvent appears to be very important to slow down the reversible process.[15a,16] In general, however, solidification of organic polymer chains results in dense, nonporous solids because such highly flexible and translationally and conformationally mobile macromolecules tend to minimize their own void volume by efficiently packing in the solid state.[15b] In addition, such polymers are mostly formed under kinetic control and irreversible conditions; hence, the formed bonds hardly rearrange into the ideal positions to achieve highly porous and ordered structures. Consequently, molecules with high rigidity and symmetry, nonplanarity, and high connectivity have been considered as suitable monomers that can frustrate the packing of the resulting polymers, and thus afford loosely packed, porous solids. Polymers of intrinsic microporosity (PIMs) formed by means of dioxane-forming reactions exhibit apparent Brunauer–Emmet–Teller (BET) specific surface areas of 500–1000 $m^2 g^{-1}$ depending on the structure of the monomers.[17] Hyper-cross-linked polymers are another example of porous organic polymers that can display permanent porosity because of extensive chemical cross-links that prevent the polymer chains collapsing into dense solids.[18] The simplest networks constructed from styrenic monomers have a wide range of BET surface areas (100–2000 $m^2 g^{-1}$) that depend mainly on the degree of cross-linking and the monomers. Amorphous conjugated microporous polymers can be synthesized with BET surface areas in the range 500–1200 $m^2 g^{-1}$ by means of Pd^0/Cu^I-catalyzed Sonogashira cross-coupling.[19] Micropore distributions of these conjugated poly(arylene ethynylene) materials could be controlled by means of the rigid node–strut topology, in particular by the average strut length,[19a,b] and this implies that order and crystallinity are not prerequisites for precise control over porosity of materials. These previous reports strongly suggest that selection of the right monomer is a critical factor to achieve synthetic porous organic polymers with high surface area and narrow pore size distribution.

As pores in solid polymers can be constructed by extensively cross-linking rigid and nonplanar monomers, D4R units were selected as starting building blocks for synthesizing porous hybrid polymers due to their rigidity, cubic shape, and highly connectable terminal groups. Moreover, the presence of D4R units in the porous networks can provide thermal stability and opportunities for further functionalization by post-synthetic methods. In contrast to the formation of siloxane networks as in sol–gel-derived silica, directly connecting the D4R siloxane cages through rigid organic linkers was considered as an alternative way to achieve porous siloxane-based materials with high surface area. We report herein inorganic–organic hybrid microporous materials synthesized by cross-coupling or copolymerization of D4R cages and rigid organic linkers. In particular, poly(ethynylene aryleneethenylene silsesquioxane) networks, simply termed polyorganosiloxane networks (PSNs), have been synthesized by Sonogashira cross-coupling of bromophenylethenyl-terminated cubic D4R siloxane cages (**BrPh-D4R**) with di/triethynyl compounds **1**–**3** (see Figure 1). The obtained PSN hybrids exhibit comparatively high thermal stability and surface area. We also found that the length and the connectivity of the ethynyl compounds affect surface areas of the PSN materials (850–1040 $m^2 g^{-1}$ BET). Utilization of these materials as potential media for hydrogen storage has also been examined.

Results and Discussion

Our attempts at targeted design of networks started with the choice of suitable building units and a coupling reaction with an effective catalyst. Figure 1 summarizes general aspects of our design: D4R cages with haloaryl terminal groups are versatile, highly connectable units for formation of inorganic–organic hybrid polymers by means of well-developed cross-coupling reactions, for example, Heck reaction, Suzuki coupling, and Sonogashira coupling.[23] Compound **BrPh-D4R** was chosen because it can be synthesized on a practical scale with high regio- and stereoselectivity by state-of-the-art cross-metathesis.[24] As D4R cages resemble the secondary building units of several crystalline zeolite frameworks, linker molecules were selected by considering the default three-periodic nets that have practically been used to design crystalline framework materials including COFs.[25] As mentioned above, however, it is nearly impossible to achieve polymer networks with long-range order, since most of them are formed under kinetic control. As a result, the three-periodic nets serve as merely qualitative guides to ideal structures. Three zeolite topologies (ACO, AFY, and LTA) can be built from D4R cages as the sole secondary building units. In their frameworks, the D4R cages are connected through two-coordinate linear linkers; the only difference is the orientation of the D4R cages. Considering the periodic arrangement of the discrete cages in

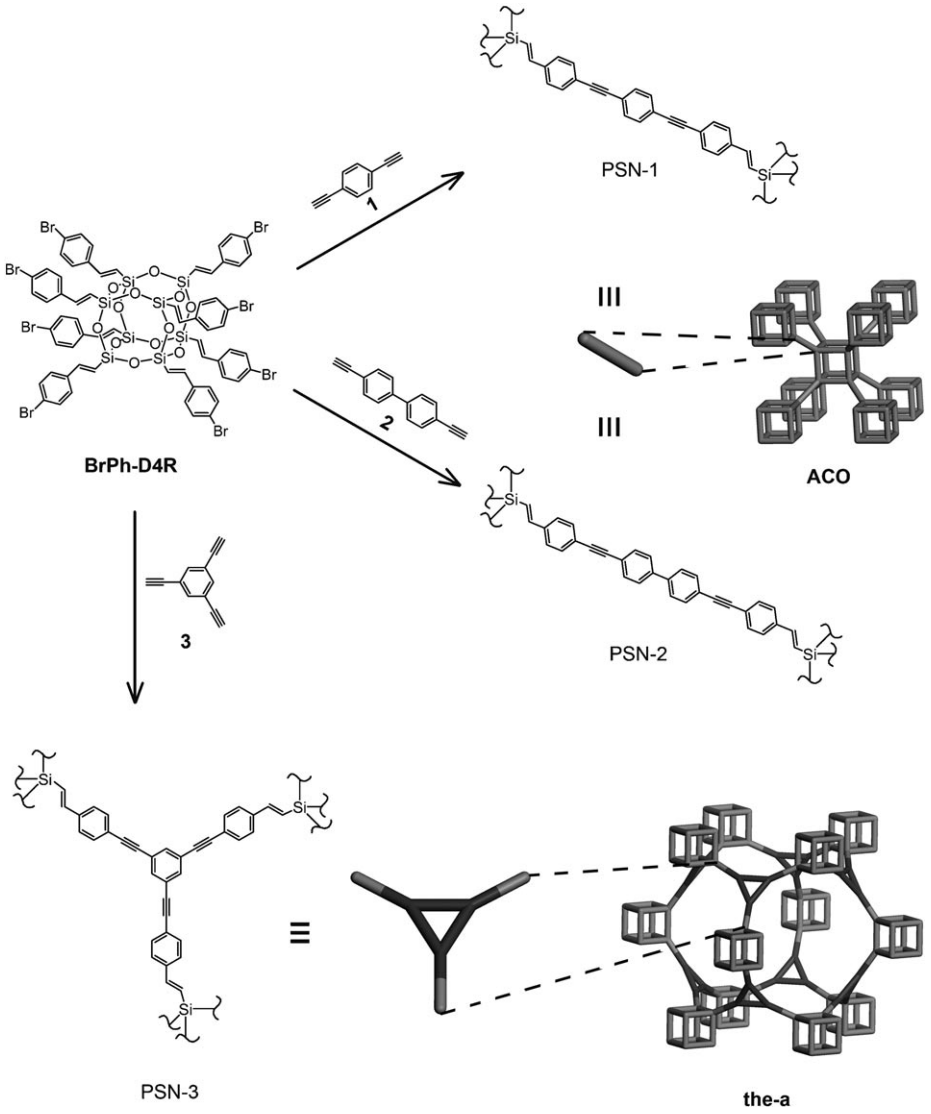

Figure 1. Design principle of poly(organosiloxane) networks (PSNs). The networks are formed by Sonogashira cross-coupling reaction with Na_2PdCl_4/[tBu$_3$PH]BF_4/CuI catalyst. Linking eight-coordinate cubes with two-coordinate linkers and three-coordinate triangles affords **ACO** topology and **the-a** net, respectively, as ideal structures.

such frameworks, the maximum symmetry of the ACO topology can be constructed from 180° linear linkers without the need to rotate the D4R cages, and thus ACO appears to be the default topology. Accordingly, one can expect connection of the D4R cages with rigid, linear molecules (e.g., **1** and **2**) to lead networks with local **ACO**-like structure.

Linkage of the cubes with shapes other than the linear ditopic linker can be described as the edge-transitive bimodal nets.[25b] If the D4R cages are regarded as cubelike vertices, connecting them through three-coordinate triangles, four-coordinate squares, four-coordinate tetrahedra, and eight-coordinate octahedra results in augmentation of the edge-transitive nets **the**; **scu** and **sqc**; **flu**; and **ocu**, respectively. Among them, the augmented form of the net (denoted **the-a**) is of particular interest to us because it has the lowest density,[25c] and rigid three-coordinate triangular molecules such as **3** are commercially available. Considering the developed active catalysts, the scope and availability of reactants, the rigidity of the resulting bonds, and the need for inorganic and/or organic bases, we selected Sonogashira coupling from among Pd-catalyzed cross-coupling reactions. The Sonogashira coupling reaction can be described as the reaction of terminal acetylenes with aryl or vinyl halides to produce internal alkynes (formation of carbon(sp)–carbon(sp^2) bonds).[26]

The most commonly used precatalysts for the Sonogashira reaction include [$PdCl_2(PPh_3)_2$], $PdCl_2$/PPh_3, and [$Pd(PPh_3)_4$] with CuI as cocatalyst, which are effective for very reactive organic halides (e.g., vinyl and aryl iodides).[23] We first utilized the [$Pd(PPh_3)_4$]/CuI catalyst to synthesize PSNs, and obtained PSN-1 to PSN-3 from the cross-coupling of **BrPh-D4R** with **1**–**3**, respectively. Progress of the reaction was evaluated by means of the residual amount of bromine. Energy-dispersive X-ray fluorescence spectroscopic data revealed that the Br/Si molar ratio of the obtained PSNs (after 48 h of the reaction; see details in the Experimental Section) was about 0.55, which corresponds to 45% conversion of phenyl bromides. As aryl bromides are less reactive electrophiles in Sonogashira coupling, a more active catalyst is needed. Palladium catalysts incorporating sterically demanding, electron-rich phosphines can furnish unusually high reactivity in a wide spectrum of coupling reactions.[23,26b–d] In particular, PtBu$_3$ and bis(1-adamantyl)benzylphosphine ((1-Ad)$_2$PBn) have proved to be exceptionally effective ligands for the Sonogashira reaction.[26c,d] Therefore, we tested Na_2PdCl_4/[tBu$_3$PH]BF_4/CuI as precatalyst for our system.[26d] The phosphonium salt was used as a ligand precursor because it is insensitive toward oxidation and hence easily handled.[26e] The Br/Si molar ratios of PSN-1 to PSN-3 obtained with the Na_2PdCl_4/[tBu$_3$PH]BF_4/CuI precatalyst were 0.13, 0.09, and 0.08, respectively, which suggests that less than one phenyl bromide moiety per D4R cage was left in the polymer networks. Thus, the present catalytic system was effective enough for constructing the PSNs. To

investigate the effects of the length and connection points of the ethynyl compounds on physicochemical properties of the resulting PSNs, all reactions were carried out under the same conditions (concentration of the D4R compound, catalyst loading, reaction temperature and time, and molar ratio of ethynyl to aryl bromide groups).

Success in the cross-coupling reaction was also confirmed by solid-state ^{1}H–^{13}C cross-polarization magic-angle spinning (CP/MAS) NMR analysis (Figure 2). The signals arising

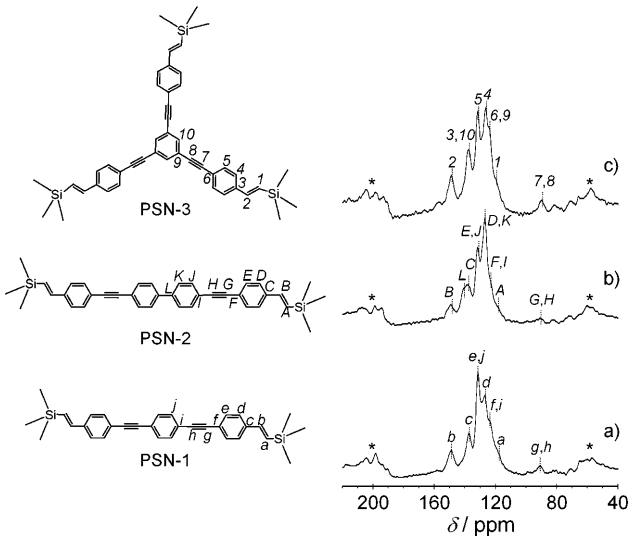

Figure 2. Solid-state ^{1}H–^{13}C CP/MAS NMR spectra of a) PSN-1, b) PSN-2, and c) PSN-3. Asterisks denote spinning side bands.

from sp-hybridized $C_{AR}C{\equiv}CC_{AR}$ carbon atoms are observed at $\delta \approx 90$ ppm, and thus confirm formation of internal carbon–carbon triple bonds. A further two small signals at $\delta = 76.3$ and 81.3 ppm are ascribed to unchanged ethynyl groups ($C_{AR}C{\equiv}CH$ and $C_{AR}C{\equiv}CH$, respectively). Note that the molar ratio of ethynyl to phenyl bromide groups was fixed at 1.5. Due to the low intensity of these signals, it is difficult to estimate the degree of homocoupling of the ethynyl compounds; the resonances attributed to the butadiynylene carbon atoms ($C{\equiv}C{-}C{\equiv}C$) overlap somewhat with those originating from the unconverted ethynyl end groups.[27] The signals around $\delta = 119$ and 149 ppm can be assigned to ethenylene carbon atoms (Si*C*H=CH and SiCH=*C*H, respectively). The resonances arising from sp^2 phenylene carbon atoms can be ascribed as shown in Figure 2.

Solid-state ^{29}Si MAS NMR analysis gave us information about the molecular structure of the D4R cages. The ^{29}Si MAS NMR spectra of the PSNs are shown in Figure 3. The spectra of all of the PSNs reveal three signals at $\delta = -61$, -68, and -76 ppm that can be assigned to T^1, T^2, and T^3 units, respectively (T^n: $CSi(OSi)_n(OH)_{3-n}$). Compared with the solution-state ^{29}Si NMR spectrum of **BrPh-D4R**, which shows a sharp resonance at $\delta = -78.49$ ppm (Figure 3a), the appearance of T^1 and T^2 units indicates that parts of the D4R cages collapsed during synthesis. The relative intensity

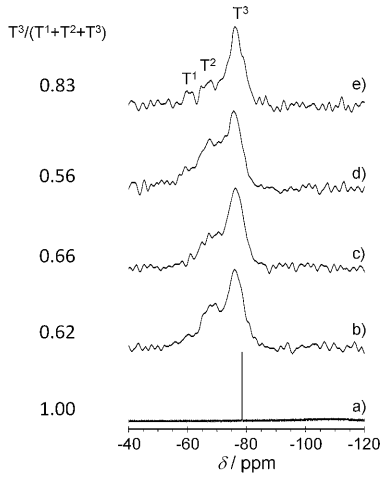

Figure 3. a) Liquid-state ^{29}Si NMR spectrum of **BrPh-D4R**. Solid-state ^{29}Si MAS NMR spectra of b) PSN-1, c) PSN-2, d) PSN-3 synthesized with Na_2PdCl_4/[tBu$_3$PH]BF_4/CuI catalyst, and e) PSN-3 synthesized with [Pd(PPh$_3$)$_4$]/CuI catalyst.

ratios of the T^3 signal, $T^3/(T^1+T^2+T^3)$, are summarized in Figure 3. The fractions of cleaved siloxane bonds of PSN-1, PSN-2, and PSN-3 were calculated from the intensity of the signals to be 15.7, 13.0, and 18.2%, respectively. Quantitative determination of the amount of D4R units remaining in the PSNs based on only spectroscopic results is very difficult; however, the degree of siloxane cleavage qualitatively suggests that statistically D4R units remain in the final products. The amounts of the remaining D4R units can be precisely evaluated by advanced X-ray analysis together with calculation of the pair distance distribution function. Although amine must be added as base in the Sonogashira reaction, special care was taken to minimize contamination with water (and also oxygen), which can cause the cleavage of siloxane bonds. Previous reports on the functionalization of D4R molecules by several cross-coupling reactions claimed that D4R cages were retained during the reactions.[13d–f,14d,24b] Since the arylene ethynylene groups are rigid and straight moieties, random connection of the rigid D4R cages with such groups could cause structural constraints or stresses. Hence, distortion of the D4R cages presumably occurred to relax the whole networks. This speculation is supported by the fact that the PSN samples synthesized by the less effective [Pd(PPh$_3$)$_4$]/CuI cross-coupling catalyst show less cleavage of siloxane bonds (only 5.8% for PSN-3; Figure 3e). We reasoned that less effective cross-coupling resulted in less distortion of the siloxane cages, and thus a lower degree of cleavage of siloxane bonds. Also, the atomistic optimization of PSN-1, as illustrated in Figure S1 in the Supporting Information, substantiates our speculation. The phenyleneethynylene groups present in the structure of PSN-1 must bend somewhat to connect the cages together. To reduce such bending, the D4R cages would be distorted, and partial cleavage of the siloxane bonds subsequently results. Distortion of the siloxane cages was also experimentally observed both in molecular crystals and in extended crys-

talline frameworks.[28] In zeolite frameworks, for instance, to realize the topology with desired symmetry, the Si-O-Si bond angles must be limited to a (narrow) specific range that occasionally results in the distorted cages. In other words, to keep the Si-O-Si bond angles within the possible range, the structure must rearrange to lower symmetry.[28a] Accordingly, we anticipated that partial cleavage of the siloxane bonds is mainly due to the distortion of the D4R cages gradually occurring as the polymerization reaction proceeds.

Thermal behavior and stability of the PSN materials were examined by thermogravimetric/differential thermal analyses (TG-DTA) in the presence and absence of gaseous oxygen. The TG-DTA curves of all of the PSN samples displayed in Figure 4 are very similar. In the presence of oxygen (10% O_2/90% He atmosphere), slight increases in TG weights starting around 260 °C are observed before a drastic decrease. In the pure He atmosphere, on the contrary, TG weights are constant until about 360 °C, where decreases in TG weights are observed. Since no increases in TG weight occur in the pure He atmosphere, these events are presumably due to oxidation of the PSNs, particularly the unsaturated carbon–carbon bonds. The PSNs are stable up to around 360 °C, which is comparable to porous organic polymers reported thus far.[17–22] The ceramic yields of the PSN samples (23.2, 24.8, and 18.3% for PSN-1, PSN-2, and PSN-3, respectively) are also consistent with the amounts of inorganic siloxane cages present in the networks.

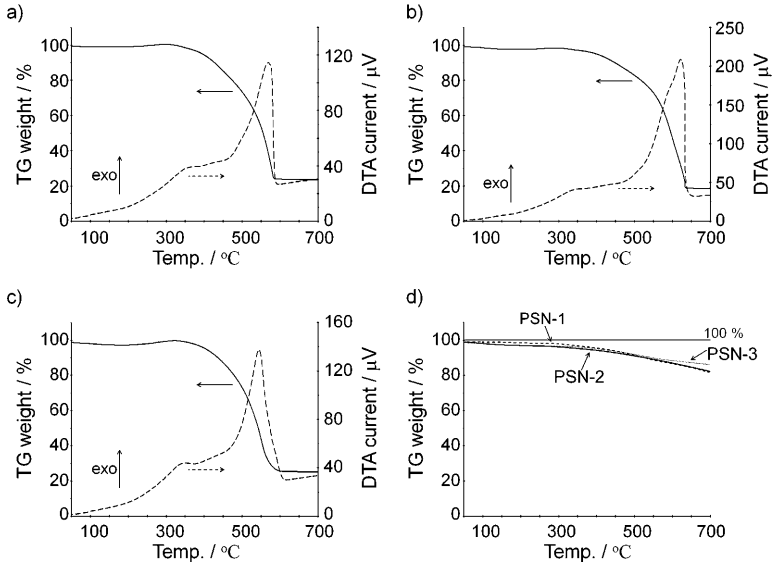

Figure 4. TG/DTA curves measured in the presence of oxygen of a) PSN-1, b) PSN-2, and c) PSN-3. d) TG curves recorded under pure He atmosphere.

As expected, the PSNs were amorphous; no long-range crystallographic order was observed in powder X-ray diffraction patterns (see Figure S2 in the Supporting Information). Particle size and morphology were observed by a field emission scanning electron microscope (FESEM). As shown in Figure 5a, PSN-1 has an irregular shape with a size of 50–80 μm. PSN-2 and PSN-3 exhibit similar morphology and particle size (see Figure S3 in the Supporting Information). Further investigations on texture and ordering of the PSNs were performed by transmission electron microscopy (TEM). The PSN samples were very stable under the electron beam. High-resolution TEM images of the PSNs are shown in Figure 5b–d. The translucent TEM images are indicative of porous, not dense, structures of the materials. No evidence of ordering is observed; however, pore diameters are relatively uniform.

To directly prove the porous character of the PSNs, nitrogen adsorption was performed. Figure 6a shows nitrogen adsorption–desorption isotherms of the PSN samples measured at 77 K. The samples show IUPAC type I isotherms with sharp uptakes at low relative pressure ($P/P_o < 0.1$) and gradual uptakes at higher relative pressure ($P/P_o > 0.1$), which indicate that they are in general microporous materials with wide meso- and macropores. The small hysteresis observed in PSN-2 may be attributed to the diffusion constraints and its framework flexibility.[29] The apparent BET specific surface areas of PSN-1, PSN-2, and PSN-3 were calculated to be 846 ± 41, 1042 ± 35, and $982 \pm 70\ m^2\,g^{-1}$, respectively. Total pore volumes (at $P/P_o = 0.99$) were 0.79 ± 0.04, 0.87 ± 0.09, and $0.86 \pm 0.06\ cm^3\,g^{-1}$, respectively. Note that these values are averages of at least three different samples synthesized from different batches under exactly the same conditions,

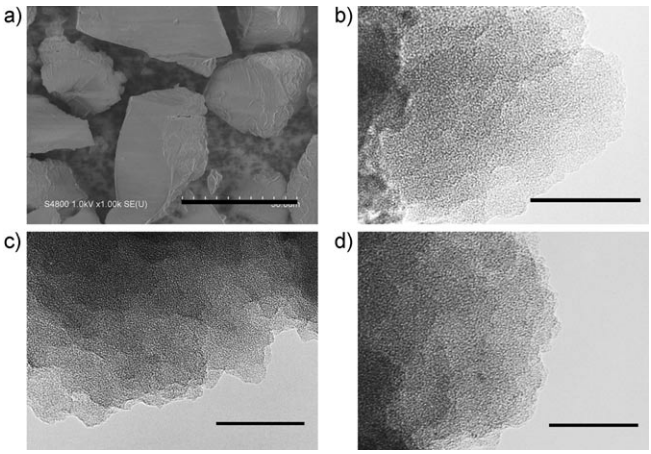

Figure 5. a) FESEM image of PSN-1 (scale bar: 50 μm). High-resolution TEM images of b) PSN-1, c) PSN-2, and d) PSN-3 (scale bar: 50 nm).

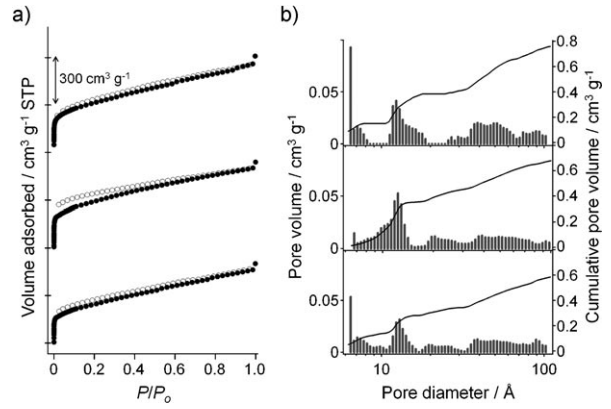

Figure 6. a) Nitrogen adsorption–desorption isotherms of PSN-1 (bottom), PSN-2 (middle), and PSN-3 (top). Filled and empty symbols denote adsorption and desorption branches, respectively. For clarity the isotherms of PSN-2 and PSN-3 are shifted vertically by 600 and 1200 $cm^3 g^{-1}$, respectively. b) NLDFT pore size distribution (left axis) and cumulative pore volume (right axis) of PSN-1 (bottom), PSN-2 (middle), and PSN-3 (top).

whereby each sample was measured twice. The PSN samples synthesized with the $[Pd(PPh_3)_4]$/CuI catalyst, which results in less effective cross-coupling, exhibit lower BET surface areas (about 70–80% of those synthesized with the Na_2PdCl_4/$[tBu_3PH]BF_4$/CuI catalyst). These results confirmed that the efficiency in cross-linking strongly influences the surface area of the resulting networks.

Due to the disordered nature of the PSNs, accurate determination of the pore size distributions of the samples is very difficult; calculations by different methods give different values. However, the calculated results can give us qualitative information, and allow comparison of materials synthesized from different monomers. Nonlocal density functional theory (NLDFT) was employed to evaluate the pore size distributions of the materials (Figure 6b). PSN-1 and PSN-3 exhibit bimodal pore diameters of about 7 and 12 Å, whereas PSN-2 has a pore diameter of about 12 Å. For materials built from ditopic ethynyl molecules of different lengths, that is, PSN-1 and PSN-2, the pore size distribution tends to be shifted to larger pore diameter with increasing length of the linker molecules. As PSN-3 has a more uniform pore size distribution than PSN-1, the three-connecting linkers locally connect the D4R cages more rigidly and orderly than the two-connecting ones. The calculated pore sizes of PSN-1 were about one-half and one-third of the ideal diameter modeled on the basis of the **ACO** topology by atomistic simulation (see the Supporting Information), which suggests that the PSNs are catenation-like networks. As is often observed in crystalline frameworks,[30] interpenetration or interweaving of two or more independent and identical frameworks occurs when the length of strut or ligand is too long, as such catenated structures form to minimize void space or to maximize packing efficiency. In the case of amorphous polymeric materials, catenation-like frameworks are likely a result of interpenetration of nonidentical but similar networks.[30a]

Low-density organic microporous materials such as PIMs,[17b] hyper-cross-linked polymers,[18b–d] and conjugated microporous polymers[19b] have been studied as potential media for hydrogen storage. The PSNs are also of interest for this application. To evaluate their potential, hydrogen adsorption was performed by a volumetric method at 77 and 87 K. Figure 7 shows hydrogen adsorption isotherms of the

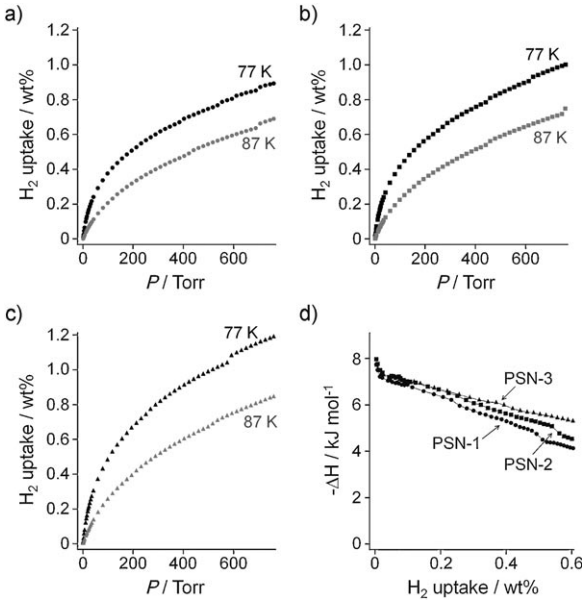

Figure 7. Hydrogen adsorption isotherms measured at 77 (black) and 87 K (gray) of a) PSN-1, b) PSN-2, and c) PSN-3. d) Isosteric heats of hydrogen adsorption.

PSN samples and their corresponding isosteric heats of adsorption. Hydrogen uptakes by PSN-1, PSN-2, and PSN-3 at 77 K and 760 Torr are 0.89, 1.00, and 1.19 wt%, respectively. Thus, the PSNs outperform inorganic mesoporous silicas,[31] and are comparable to microporous zeolites[32] and porous organic polymers.[17b,18b–d,19b] The isosteric heats of adsorption at low hydrogen coverage for PSN-1, PSN-2, and PSN-3 were calculated to be 7.7, 8.0, and 7.7 kJ mol^{-1}, respectively. Their isosteric heats of adsorption decrease monotonically with increasing surface coverage of hydrogen, and this suggests that the surface, or more specifically the interaction, available for hydrogen adsorption is rather heterogeneous. The relatively high isosteric heats of adsorption for the PSNs are comparable to those of several good candidates for hydrogen storage media, including porous organic polymers[17b,18b–d,19b] and metal–organic frameworks.[33] The primary binding sites are likely organic aromatic and ethynyl groups, since π-electron systems can exhibit relatively high interaction energies with hydrogen molecules.[18b,19b,34] Silanol and siloxane groups are responsible for adsorption at higher loading. Because the presence of palladium in porous materials has a positive impact on hydrogen storage through a spillover mechanism,[35] effects of residual palladium (the residual amount could not be detected by an energy-disper-

sive X-ray fluorescence spectrometer) on such high enthalpies of adsorption must be considered. As previously reported for porous polymers synthesized by palladium-catalyzed reactions, no clear relation between residual amounts of palladium and heats of adsorption was observed.[18b,19b] In addition, spillover is not expected to be responsible for adsorption at low pressure and cryogenic temperatures.[35] We thus consider that the observed heats of adsorption arise directly from the chemical functionality of the PSN materials.

With regard to achieving the U.S. Department of Energy targets for hydrogen storage systems (revised targets: 0.045 kg H_2/kg system by 2010; 0.055 kg H_2/kg system by 2015),[36] the PSNs must be engineered to increase accessible surface areas while keeping relatively uniform micropores. Also, design and functionalization of the networks are of vital importance to gain higher heats of adsorption. Organic parts of the PSNs can be functionalized with electron-donating groups to increase the strength of hydrogen–PSN interactions.[34b] Although the siloxane bonds were partially cleaved during synthesis, we consider, based on the degree of cleavage, that the D4R cages are at least partly retained in the PSNs. The presence of the D4R cages and the silanol groups in the PSNs can offer unique properties for these hybrids over organic polymers. Hydroxyl groups can serve as selective sites for metal complexation and cation addition to enhance hydrogen adsorption.[37] In addition, as the D4R cages can trap very small species such as atomic hydrogen and fluoride ion,[38] post-synthetic incorporation of fluoride ions into the PSNs would lead to anionic porous polymeric hybrids.[38d] Specific metal cations can further be incorporated selectively into the resulting anionic PSN hybrids. Investigations on such post-synthetic modifications and their effects on hydrogen adsorption are underway.

Conclusion

Porous inorganic–organic hybrid materials have been synthesized by directly linking bromophenylethenyl-terminated cubic siloxane cages with ethynyl compounds by Sonogashira cross-coupling. In comparison with porous organic polymers reported previously, the resulting hybrid materials exhibit relatively high surface areas and comparable thermal stability. The length and connectable sites of the ethynyl compounds strongly influence the BET surface areas and the micropore size distribution. The degree of cross-linking affects the BET surface area of the obtained samples and, more importantly, the degree of cleavage of the siloxane bonds. Partial collapse of the D4R cages is considered to be mainly due to distortion of the cages. These novel materials also show comparably high hydrogen uptakes and relatively high isosteric heats of hydrogen adsorption. The presence of sp- and sp^2-carbon atoms, silanol groups, and D4R siloxane cages in these hybrid materials can be useful for further post-synthetic modifications, especially incorporation of metal complexes and cations to enhance gas adsorption.

Experimental Section

General: All reactions were carried out under nitrogen atmosphere by standard Schlenk techniques. All organic solvents were purchased from Wako Pure Chemical Industries in dehydrated grade and used as received, unless otherwise noted. Other chemicals were obtained from Wako Pure Chemical Industries, Tokyo Chemical Industry, or Sigma-Aldrich, and used without further purification. Syntheses of **BrPh-D4R** and **2** are described in the Supporting Information.

Synthesis of porous siloxane networks (PSN-*n*): An oven-dried Schlenk flask was charged with **BrPh-D4R** (0.3 g, 0.16 mmol), ethynyl compound (0.96 mmol for **1** and **2**; 0.64 mmol for **3**), sodium tetrachloropalladate(II) (11 mg, 0.038 mmol), tri-*tert*-butylphosphonium tetrafluoroborate (22 mg, 0.77 mmol), and copper(I) iodide (5 mg, 0.026 mmol). When $[Pd(PPh_3)_4]$/CuI was used as catalyst, tetrakis(triphenylphosphine)palladium(0) (18 mg, 0.016 mmol) and copper(I) iodide (6 mg, 0.032 mmol) were added instead. The flask was equipped with a condenser and a magnetic stirring bar, evacuated and re-filled with nitrogen (at least five evacuation/refilling cycles). THF (35 mL) and triethylamine (5 mL) were injected by syringe into the flask under nitrogen. The resulting solution was vigorously stirred at room temperature for 1 h to ensure in situ generation of phosphine; then the temperature was raised to 70 °C. After stirring at this temperature for 48 h, the mixture was cooled to room temperature. The polymer network was isolated by filtration and washed with THF, hexane, acetone, methanol, and dichloromethane to remove any amine salts, unconsumed monomers, and catalyst residues. Further purification of the sample was carried out by extraction with THF at 60 °C. The product was recovered by filtration, and dried under reduced pressure at 60 °C.

Atomistic simulation: Molecular models for the PSNs were generated out by creating fragments of networks based on the **ACO** topology or **the-a** net with Materials Studio 4.4 (Accelrys Software Inc.). All models were optimized by using the Discovery module with the cvff force field.

Characterization: Solution-state NMR spectra were recorded on a Jeol JNM-EX-270 spectrometer at 270.0 MHz for ^1H, 67.80 MHz for ^{13}C, and 53.45 MHz for ^{29}Si. Chemical shifts are reported in ppm downfield from $SiMe_4$. Solid-state NMR spectra were obtained on a Chemagnetics CMS-300 spectrometer. ^{29}Si MAS NMR spectra were recorded at 59.7 MHz with a pulse width of 2.0 μs and a recycle delay of 80 s, while ^1H–^{13}C CP MAS NMR spectra were recorded at 75.6 MHz with a contact time of 1.5 ms and a recycle delay of 5 s. Residual amounts of bromine and palladium were determined by energy-dispersive X-ray fluorescence spectroscopy (Jeol JSX-3400RII). TG/DTA was performed on a PU 4K (Rigaku) at a heating rate of 10 K min^{-1} with 10 % O_2/90 % He or pure He as carrier gas. Powder XRD patterns were collected on an M03X-HF (Bruker AXS) with $Cu_{K\alpha}$ radiation (40 kV, 30 mA). Size and morphology of the samples were observed under a field-emission scanning electron microscope (Hitachi S-4800). Transmission electron microscopy (TEM) was carried out on a Jeol JEM 2000EXII operated at 200 kV. Volumetric gas adsorption was performed on an Autosorb-1 instrument (Quantachrome). Nitrogen and hydrogen adsorption isotherms at 77 K were measured in liquid-nitrogen baths, while hydrogen adsorption isotherms at 87 K were measured in liquid-argon baths. Research or special grades of gases (99.9995 % for H_2, 99.99995 % for N_2 and He) were used throughout the adsorption experiments. Before the measurement, the samples were degassed at 120 °C and 10 Pa for at least 8 h. Pore size distribution was calculated by a nonlocal density functional theory (NLDFT) by using the carbon slit/cylindrical pore model.

Acknowledgements

We thank Mr. T. Moteki and Mr. M. Kubo for their technical assistance in the FESEM observations and the gas adsorption measurements, respectively, and Prof. S. Maruyama for access to the FESEM instrument. A part of this work was conducted in Center for Nano Lithography & Analysis, The University of Tokyo, supported by the Ministry of Educa-

tion, Culture, Sports, Science and Technology (MEXT), Japan. This work was supported in part by a Grant-in-Aid for Scientific Research (B), the Japan Society for the Promotion of Science (JSPS), and by Global COE program (Mechanical Systems Innovation), MEXT, Japan.

[1] a) D. W. Breck, *Zeolite Molecular Sieves*, Wiley, New York, **1974**; b) M. E. Davis, *Nature* **2002**, *417*, 813–821.

[2] C. J. Brinker, G. W. Scherer, *Sol-Gel Science*, Academic Press, San Diego, **1990**.

[3] a) C. W. Jones, K. Tsuji, M. E. Davis, *Nature* **1998**, *393*, 52–54; b) Y. Wada, T. Okubo, M. Ryo, T. Nakazawa, Y. Hasegawa, S. Yanagida, *J. Am. Chem. Soc.* **2000**, *122*, 8583–8584; c) W. Chaikittisilp, M. E. Davis, T. Okubo, *Chem. Mater.* **2007**, *19*, 4120–4122.

[4] a) T. Wakihara, T. Okubo, *Chem. Lett.* **2005**, *34*, 276–281; b) P. P. E. A. de Moor, T. P. M. Beelen, B. U. Komanschek, L. W. Beck, P. Wagner, M. E. Davis, R. A. van Santen, *Chem. Eur. J.* **1999**, *5*, 2083–2088; c) T. M. Davis, T. O. Drews, H. Ramanan, C. He, J. Dong, H. Schnablegger, M. A. Katsoulakis, E. Kokkoli, A. V. Mccormick, R. L. Penn, M. Tsapatsis, *Nat. Mater.* **2006**, *5*, 400–408.

[5] a) A. W. Burton, *J. Am. Chem. Soc.* **2007**, *129*, 7627–7637; b) W. Fan, S. Shirato, F. Gao, M. Ogura, T. Okubo, *Microporous Mesoporous Mater.* **2006**, *89*, 227–234.

[6] a) Y. Wan, D. Zhao, *Chem. Rev.* **2007**, *107*, 2821–2860; b) J. S. Beck, J. C. Vartuli, W. J. Roth, M. E. Leonowicz, C. T. Kresge, K. D. Schmitt, C. T.-W. Chu, D. H. Olson, E. W. Sheppard, S. B. McCullen, J. B. Higgins, J. L. Schlenker, *J. Am. Chem. Soc.* **1992**, *114*, 10834–10843; c) M. Ogura, H. Miyoshi, S. P. Naik, T. Okubo, *J. Am. Chem. Soc.* **2004**, *126*, 10937–10944.

[7] a) G. J. A. A. Soler-Illia, P. Innocenzi, *Chem. Eur. J.* **2006**, *12*, 4478–4494; b) F. Hoffmann, M. Cornelius, J. Morell, M. Fröba, *Angew. Chem.* **2006**, *118*, 3290–3328; *Angew. Chem. Int. Ed.* **2006**, *45*, 3216–3251.

[8] a) R. M. Laine, *J. Mater. Chem.* **2005**, *15*, 3725–3744; b) R. E. Morris, *J. Mater. Chem.* **2005**, *15*, 931–938.

[9] a) G. Fu, C. A. Fyfe, W. Schwieger, G. T. Kokotailo, *Angew. Chem.* **1995**, *107*, 1582–1585; *Angew. Chem. Int. Ed. Engl.* **1995**, *34*, 1499–1502; b) C. A. Fyfe, G. Fu, *J. Am. Chem. Soc.* **1995**, *117*, 9709–9714; c) L. Zhang, H. C. L. Abbenhuis, Q. Yang, Y.-M. Wang, P. C. M. M. Magusin, B. Mezari, R. A. van Santen, C. Li, *Angew. Chem.* **2007**, *119*, 5091–5094; *Angew. Chem. Int. Ed.* **2007**, *46*, 5003–5006.

[10] a) C. Zhang, F. Babonneau, C. Bonhomme, R. M. Laine, C. L. Soles, H. A. Hristov, A. F. Yee, *J. Am. Chem. Soc.* **1998**, *120*, 8380–8391; b) J. J. Morrison, C. J. Love, B. W. Manson, I. J. Shannon, R. E. Morris, *J. Mater. Chem.* **2002**, *12*, 3208–3212.

[11] a) Y. Hagiwara, A. Shimojima, K. Kuroda, *Chem. Mater.* **2008**, *20*, 1147–1153; b) H. Kuge, Y. Hagiwara, A. Shimojima, K. Kuroda, *Chem. Asian J.* **2008**, *3*, 600–606.

[12] a) A. Shimojima, R. Goto, N. Atsumi, K. Kuroda, *Chem. Eur. J.* **2008**, *14*, 8500–8506; b) R. Goto, A. Shimojima, H. Kuge, K. Kuroda, *Chem. Commun.* **2008**, 6152–6154.

[13] a) P. G. Harrison, *J. Organomet. Chem.* **1997**, *542*, 141–183; b) B. W. Manson, J. J. Morrison, P. I. Couper, P.-A. Jaffrès, R. E. Morris, *J. Chem. Soc. Dalton Trans.* **2001**, 1123–1127; c) K. Naka, M. Fujita, K. Tanaka, Y. Chujo, *Langmuir* **2007**, *23*, 9057–9063; d) C. M. Brick, Y. Ouchi, Y. Chujo, R. M. Laine, *Macromolecules* **2005**, *38*, 4661–4665; e) M. Z. Asuncion, M. F. Roll, R. M. Laine, *Macromolecules* **2008**, *41*, 8047–8052; f) M. F. Roll, M. Z. Asuncion, J. Kampf, R. M. Laine, *ACS Nano* **2008**, *2*, 320–326.

[14] a) R. Duchateau, *Chem. Rev.* **2002**, *102*, 3525–3542; b) F. Carniato, C. Bisio, E. Boccaleri, M. Guidotti, E. Gavrilova, L. Marchese, *Chem. Eur. J.* **2008**, *14*, 8098–8101; c) D. Neumann, M. Fisher, L. Tran, J. G. Matisons, *J. Am. Chem. Soc.* **2002**, *124*, 13998–13999; d) M. Y. Lo, C. Zhen, M. Lauters, G. E. Jabbour, A. Sellinger, *J. Am. Chem. Soc.* **2007**, *129*, 5808–5809; e) F. Carniato, C. Bisio, G. Gatti, E. Boccaleri, L. Bertinetti, S. Coluccia, O. Monticelli, L. Marchese, *Angew. Chem.* **2009**, *121*, 6175–6177; *Angew. Chem. Int. Ed.* **2009**, *48*, 6059–6061; f) J. M. Mabry, A. Vij, S. T. Iacono, B. D. Viers, *Angew. Chem.* **2008**, *120*, 4205–4208; *Angew. Chem. Int. Ed.* **2008**, *47*, 4137–4140.

[15] a) M. Mastalerz, *Angew. Chem.* **2008**, *120*, 453–455; *Angew. Chem. Int. Ed.* **2008**, *47*, 445–447; b) C. Weder, *Angew. Chem.* **2008**, *120*, 456–458; *Angew. Chem. Int. Ed.* **2008**, *47*, 448–450.

[16] a) A. P. Côté, A. I. Benin, N. W. Ockwig, M. O'Keeffe, A. J. Matzger, O. M. Yaghi, *Science* **2005**, *310*, 1166–1170; b) H. M. El-Kaderi, J. R. Hunt, J. L. Mendoza-Cortés, A. P. Côté, R. E. Taylor, M. O'Keeffe, O. M. Yaghi, *Science* **2007**, *316*, 268–272; c) J. R. Hunt, C. J. Doonan, J. D. LeVangie, A. P. Côté, O. M. Yaghi, *J. Am. Chem. Soc.* **2008**, *130*, 11872–11873; d) S. Wan, J. Guo, J. Kim, H. Ihee, D. Jiang, *Angew. Chem.* **2008**, *120*, 8958–8962; *Angew. Chem. Int. Ed.* **2008**, *47*, 8826–8830.

[17] a) P. M. Budd, B. S. Ghanem, S. Makhseed, N. B. McKeown, K. J. Msayib, C. E. Tattershall, *Chem. Commun.* **2004**, 230–231; b) N. B. McKeown, B. Gahnem, K. J. Msayib, P. M. Budd, C. E. Tattershall, K. Mahmood, S. Tan, D. Book, H. W. Langmi, A. Walton, *Angew. Chem.* **2006**, *118*, 1836–1839; *Angew. Chem. Int. Ed.* **2006**, *45*, 1804–1807; c) N. B. McKeown, P. M. Budd, K. J. Msayib, B. S. Ghanem, H. J. Kingston, C. E. Tattershall, S. Makhseed, K. J. Reynolds, D. Fritsch, *Chem. Eur. J.* **2005**, *11*, 2610–2620.

[18] a) M. P. Tsyurupa, V. A. Davankov, *React. Funct. Polym.* **2006**, *66*, 768–779; b) J. Germain, J. Hradil, J. M. J. Fréchet, F. Svec, *Chem. Mater.* **2006**, *18*, 4430–4435; c) C. D. Wood, B. Tan, A. Trewin, H. Niu, D. Bradshaw, M. J. Rosseinsky, Y. Z. Khimyak, N. L. Campbell, R. Kirk, E. Stöckel, A. I. Cooper, *Chem. Mater.* **2007**, *19*, 2034–2048; d) J. Germain, F. Svec, J. M. J. Fréchet, *Chem. Mater.* **2008**, *20*, 7069–7076.

[19] a) J.-X. Jiang, F. Su, A. Trewin, C. D. Wood, N. L. Campbell, H. Niu, C. Dickinson, A. Y. Ganin, M. J. Rosseinsky, Y. Z. Khimyak, A. I. Cooper, *Angew. Chem.* **2007**, *119*, 8728–8732; *Angew. Chem. Int. Ed.* **2007**, *46*, 8574–8578; b) J.-X. Jiang, F. Su, A. Trewin, C. D. Wood, H. Niu, J. T. A. Jones, Y. Z. Khimyak, A. I. Cooper, *J. Am. Chem. Soc.* **2008**, *130*, 7710–7720; c) J.-X. Jiang, F. Su, H. Niu, C. D. Wood, N. L. Campbell, Y. Z. Khimyak, A. I. Cooper, *Chem. Commun.* **2008**, 486–488; d) J. Weber, A. Thomas, *J. Am. Chem. Soc.* **2008**, *130*, 6334–6335; e) J. Schmidt, J. Weber, J. D. Epping, M. Antonietti, A. Thomas, *Adv. Mater.* **2009**, *21*, 702–705.

[20] a) T. Ben, H. Ren, S. Ma, D. Cao, J. Lan, X. Jing, W. Wang, J. Xu, F. Deng, J. M. Simmons, S. Qiu, G. Zhu, *Angew. Chem.* **2009**, *121*, 9621–9624; *Angew. Chem. Int. Ed.* **2009**, *48*, 9457–9460; b) H. Ren, T. Ben, E. Wang, X. Jing, M. Xue, B. Liu, Y. Cui, S. Qiu, G. Zhu, *Chem. Commun.* **2010**, *46*, 291–293.

[21] a) P. Kuhn, M. Antonietti, A. Thomas, *Angew. Chem.* **2008**, *120*, 3499–3502; *Angew. Chem. Int. Ed.* **2008**, *47*, 3450–3453; b) P. Kuhn, A. Forget, D. Su, A. Thomas, M. Antonietti, *J. Am. Chem. Soc.* **2008**, *130*, 13333–13337.

[22] a) M. Rose, W. Böhlmann, M. Sabo, S. Kaskel, *Chem. Commun.* **2008**, 2462–2464; b) E. Stöckel, X. Wu, A. Trewin, C. D. Wood, R. Clowes, N. L. Campbell, J. T. A. Jones, Y. Z. Khimyak, D. J. Adams, A. I. Cooper, *Chem. Commun.* **2009**, 212–214; c) O. K. Farha, A. M. Spokoyny, B. G. Hauser, Y.-S. Bae, S. E. Brown, R. Q. Snurr, C. A. Mirkin, J. T. Hupp, *Chem. Mater.* **2009**, *21*, 3033–3035.

[23] *Metal-Catalyzed Cross-Coupling Reactions*, 2nd ed. (Eds.: A. de Meijere, F. Diederich), Wiley-VCH, Weinheim, **2004**.

[24] a) Y. Itami, B. Marciniec, M. Kubicki, *Chem. Eur. J.* **2004**, *10*, 1239–1248; b) S. Sulaiman, A. Bhaskar, J. Zhang, R. Guda, T. Goodson III, R. M. Laine, *Chem. Mater.* **2008**, *20*, 5563–5573; c) G. Cheng, N. R. Vautravers. R. E. Morris, D. J. Cole-Hamilton, *Org. Biomol. Chem.* **2008**, *6*, 4662–4667.

[25] a) O. Delgado-Friedrichs, M. O'Keeffe, O. M. Yaghi, *Phys. Chem. Chem. Phys.* **2007**, *9*, 1035–1043; b) O. Delgado-Friedrichs, M. O'Keeffe, O. M. Yaghi, *Acta Crystallogr. Sect. A* **2006**, *62*, 350–355; c) Reticular Chemistry Structure Resource, http://rcsr.anu.edu.au/.

[26] a) K. Sonogashira, Y. Tohda, N. Hagihara, *Tetrahedron Lett.* **1975**, *16*, 4467–4470; b) G. C. Fu, *Acc. Chem. Res.* **2008**, *41*, 1555–1564; c) T. Hundertmark, A. F. Littke, S. L. Buchwald, G. C. Fu, *Org. Lett.* **2000**, *2*, 1729–1731; d) A. Köllhofer, T. Pullmann, H. Plenio, *Angew.*

Chem. **2003**, *115*, 1086–1088; *Angew. Chem. Int. Ed.* **2003**, *42*, 1056–1058; e) M. R. Netherton, G. C. Fu, *Org. Lett.* **2001**, *3*, 4295–4298.
[27] V. S.-Y. Lin, D. R. Radu, M.-K. Han, W. Deng, S. Kuroki, B. H. Shanks, M. Pruski, *J. Am. Chem. Soc.* **2002**, *124*, 9040–9041.
[28] a) M. O'Keeffe, O. M. Yaghi, *Chem. Eur. J.* **1999**, *5*, 2796–2801; b) H.-B. Buergi, K. W. Törnroos, G. Calzaferri, H. Bürgy, *Inorg. Chem.* **1993**, *32*, 4914–4919.
[29] a) T. Loiseau, C. Serre, C. Huguenard, G. Fink, F. Taulelle, M. Henry, T. Bataille, G. Férey, *Chem. Eur. J.* **2004**, *10*, 1373–1382; b) R. Kitaura, K. Seki, G. Akiyama, S. Kitagawa, *Angew. Chem.* **2003**, *115*, 444–447; *Angew. Chem. Int. Ed.* **2003**, *42*, 428–431; c) F. J. Uribe-Romo, J. R. Hunt, H. Furukawa, C. Klöck, M. O'Keeffe, O. M. Yaghi, *J. Am. Chem. Soc.* **2009**, *131*, 4570–4571.
[30] a) D. Klempner, *Angew. Chem.* **1978**, *90*, 104–113; *Angew. Chem. Int. Ed. Engl.* **1978**, *17*, 97–106; b) T. K. Maji, R. Matsuda, S. Kitagawa, *Nat. Mater.* **2007**, *6*, 142–148; c) S. Ma, D. Sun, M. Ambrogio, J. A. Fillinger, S. Parkin, H.-C. Zhou, *J. Am. Chem. Soc.* **2007**, *129*, 1858–1859.
[31] a) X.-Z. Chu, Y.-P. Zhou, Y.-Z. Zhang, W. Su, Y. Sun, L. Zhou, *J. Phys. Chem. B* **2006**, *110*, 22596–22600; b) A. I. Acatrinei, M. A. Hartl, J. Eckert, E. H. L. Falcao, G. Chertkov, L. L. Daemen, *J. Phys. Chem. C* **2009**, *113*, 15634–15638.
[32] a) A. Zecchina, S. Bordiga, J. G. Vitillo, G. Ricchiardi, C. Lamberti, G. Spoto, M. Bjørgen, K. P. Lillerud, *J. Am. Chem. Soc.* **2005**, *127*, 6361–6366; b) S. H. Jhung, J. W. Yoon, J. S. Lee, J.-S. Chang, *Chem. Eur. J.* **2007**, *13*, 6502–6507; c) F. J. Torres, J. G. Vitillo, B. Civalleri, G. Ricchiardi, A. Zecchina, *J. Phys. Chem. C* **2007**, *111*, 2505–2513.
[33] a) J. L. C. Rowsell, O. M. Yaghi, *Angew. Chem.* **2005**, *117*, 4748–4758; *Angew. Chem. Int. Ed.* **2005**, *44*, 4670–4679; b) M. Dincă, J. R. Long, *Angew. Chem.* **2008**, *120*, 6870–6884; *Angew. Chem. Int. Ed.* **2008**, *47*, 6766–6779; c) L. J. Murray, M. Dincă, J. R. Long, *Chem. Soc. Rev.* **2009**, *38*, 1294–1314.
[34] a) O. Hübner, A. Glöss, M. Fichtner, W. Klopper, *J. Phys. Chem. A* **2004**, *108*, 3019–3023; b) R. C. Lochan, M. Head-Gordon, *Phys. Chem. Chem. Phys.* **2006**, *8*, 1357–1370.
[35] a) R. T. Yang, Y. Wang, *J. Am. Chem. Soc.* **2009**, *131*, 4224–4226; b) Y. Li, R. T. Yang, *AIChE J.* **2008**, *54*, 269–279; c) L. Wang, R. T. Yang, *J. Phys. Chem. C* **2008**, *112*, 12486–12494.
[36] U.S. Department of Energy, Targets for Onboard Hydrogen Storage Systems for Light-Duty Vehicles (http://www1.eere.energy.gov/hydrogenandfuelcells/storage/current_technology.html).
[37] a) N. Chino, M. Ogura, T. Kodaira, J. Izumi, T. Okubo, *J. Phys. Chem. B* **2005**, *109*, 8574–8579; b) S. S. Han, W. A. Goddard III, *J. Am. Chem. Soc.* **2007**, *129*, 8422–8423; c) K. L. Mulfort, J. T. Hupp, *J. Am. Chem. Soc.* **2007**, *129*, 9604–9605; d) K. L. Mulfort, O. K. Farha, C. L. Stern, A. A. Sarjeant, J. T. Hupp, *J. Am. Chem. Soc.* **2009**, *131*, 3866–3868.
[38] a) R. Sasamori, Y. Okaue, T. Isobe, Y. Matsuda, *Science* **1994**, *265*, 1691–1693; b) N. Weiden, M. Päch, K.-P. Dinse, *Appl. Magn. Reson.* **2001**, *21*, 507–516; c) A. R. Bassindale, M. Pourny, P. G. Taylor, M. B. Hursthouse, M. E. Light, *Angew. Chem.* **2003**, *115*, 3612–3614; *Angew. Chem. Int. Ed.* **2003**, *42*, 3488–3490; d) S. E. Anderson, D. J. Bodzin, T. S. Haddad, J. A. Boatz, J. M. Mabry, C. Mitchell, M. T. Bowers, *Chem. Mater.* **2008**, *20*, 4299–4309.

Received: January 28, 2010
Published online: April 13, 2010

